

STRONTIUM DISTRIBUTION IN UPPER DEVONIAN CONODONT ELEMENTS: A PALAEOBIOLOGICAL PROXY

ANDREY V. ZHURAVLEV & SERGEY S. SHEVCHUK

Institute of Geology Komi SC URB RAS, 54 Pervomayskaya, Syktyvkar, 167000, Russia. E-mail: micropalaeontology@gmail.com

To cite this article: Zhuravlev A. V. & Shevchuk S. S. (2017) - Strontium distribution in Upper Devonian conodont elements: a palaeobiological proxy. *Riv. It. Paleontol. Strat.*, 123(2): 203-210.

Keywords: conodonts; hard tissue growth; bioapatite; Sr variations.

Abstract. Conodonts are an extinct group of marine animals possessing debated affinities. The conodont elements are composed of calcium phosphate [apatite (CaF)] and collagen-like proteins. Distribution of Sr in the bioapatite of albid, lamellar and paralamellar tissues of some Upper Devonian conodont element crowns from NW Russia was studied by microprobe. The calcium phosphate of the lamellar and paralamellar tissues demonstrates periodical oscillation of Sr contents across the lamellae (0.4-0.5 wt% in the outer part of lamella, and 0.2 wt% in the inner part). The albid tissue contains Sr of less than 0.4 wt%. It is suggested that oscillations of Sr concentrations reflect the periodic growth of the lamellae, and the average Ca/Sr ratio can be a proxy of the growth rate.

INTRODUCTION

Conodonts are a Palaeozoic and Triassic extinct group of marine animals possessing debated affinities (e.g. Kasatkina & Buryi 1996; Donoghue et al. 2000; Blicek et al. 2010; Turner et al. 2010). The only mineralized parts of the animals are tooth-like elements disposed in a bilaterally symmetrical apparatus having a possible feeding scope. All the conodont elements consist of two parts – crown and basal filling. The crowns are more resistant to diagenetic alteration during burial, and are therefore better preserved (Donoghue 1998; Zhuravlev 2002; Trotter & Eggins 2006) (Fig. 1).

Lamellar, paralamellar, interlamellar, albid and basal filling are the major tissues which make up the conodont element. The crown of a conodont element is composed of four of these major tissues (excluding basal filling) and covered in lamellar tissue above the basal body/crown junction (Donoghue 1998; Zhuravlev 2002).

These tissue types have different crystalline arrangement, microstructure, and organic contents (e.g. Müller & Nogami 1971; Barnes et al. 1973, 1975; Donoghue 1998; Zhuravlev 2002). Generally the hard tissues are composed of calcium phosphate [apatite (CaF)] and collagen-like proteins (Kemp

2002; Rosseeva et al. 2011; Frank-Kamenetskaya et al. 2014; Gerasimova et al. 2015; Zhuravlev & Gerasimova 2015) and slightly differ from tissues of teeth and bones of vertebrates (e.g. Blicek et al. 2010; Turner et al. 2010).

The variation of chemical composition of the conodont mineralized tissues is subject of debate (Pietzner et al. 1968; Wright 1989, 1990; Kurschner et al. 1993; Trotter et al. 1999; Trotter & Eggins 2006; Trotter et al. 2007; Rosseeva et al. 2011; Katvala & Henderson 2012) (Tab. 1). The conodont bioapatite generally contains near-primary (in vivo) and secondary (postmortem) minor admixtures comprising Na, Sr, Mg, Al, Si, S, and REE (Trotter et al. 2007; Katvala & Henderson 2012; Trotter et al. 2016). Earlier studies have been focused on the content and distribution of REE and isotope composition of Sr as a proxy of the evolution of seawater isotopic composition (Trotter et al. 1999; Trotter & Eggins 2006). Distribution of the other admixtures deemed to be near-primary (Na, S) were used for palaeobiological reconstructions as well (e.g. Katvala & Henderson 2012). It was noted that Sr concentrations are constant within the crown of Pa elements of *Mesogondolella* (Katvala & Henderson 2012), which is composed of lamellar and paralamellar tissues. Postmortem uptake was suggested for Fe, Mn, Al, Zn, REE, Pb, Th, Ba, and U (Trotter & Eggins 2006).

Received: September 19, 2016; accepted: February 16, 2017

Element	Pietzner et al. 1968	Kurschner et al. 1993	Wright 1989/This article		
			Albid tissue	Paralamellar tissue	Lamellar tissue
Ca	37.28	37.1	53.0/34.5	No data /34.7	52.5/35.1
F	2.6	No data	3.1/4.7	No data /5.2	2.8/4.5
Na	0.62	0.6044	0.1/0.2	No data /0.7	0.2/0.6
Sr	0.4	0.3121	0.4/0.2	No data /0.4	0.4/0.3

Tab. 1 - Mean composition of the unaltered conodont bioapatite (wt%)

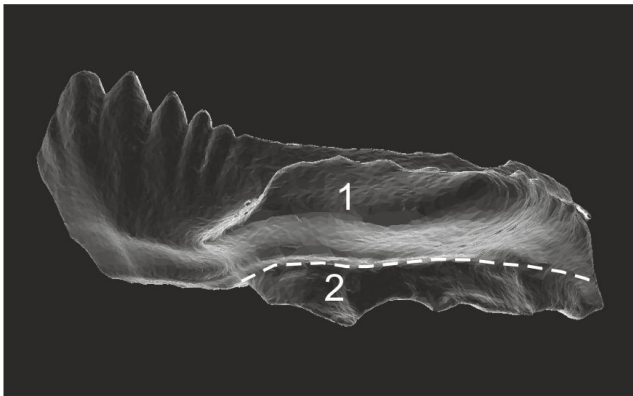


Fig. 1 - Main parts of a conodont element: 1 – crown; 2 – basal body.

The current study is focused on the distribution of Sr in various hard tissues of unaltered Upper Devonian conodont element crowns using microprobe.

MATERIAL AND METHODS

The Upper Devonian (middle Frasnian) conodont elements were collected from an outcrop located in the Novgorod region (NW Russia, N 58°11'0.2" E 31°00'50.5"), where the host rock is bioclastic clayey packstone lenses in the claystones of the Rdeyskoe Formation, Ilmen Beds (Zhuravlev et al. 1997) (Fig. 2). The lenses are believed to be calcitempestites deposited in a shallow-water epicontinental basin (Tarasenko 2011). Bulk concentration of Sr, Na, and Fe in the limestone are 0.02-0.04 wt%, 0.01-0.6 wt%, and <0.01 wt% respectively.

Biostratigraphically the studied sample corresponds to the late *Palmatolepis punctata* conodont zone or MN Zone 6 of Klapper (1997) (Zhuravlev et al. 2006). The conodont association of the sample (204 Pa, 40 Pb, 296 S, and 54 M elements) is composed of *Mehlina gradata* Youngquist, *Youngquistognathus angustidiscus* (Youngquist), *Youngquistognathus rossicus* Zhuravlev, *Polygnathus* spp., *Polygnathus alatus* Huddle, *Polygnathus aequalis* Klapper et Lane, *Polygnathus dubius* Branson et Mehl, *Polygnathus decorosus* Stauffer, *Polygnathus ilmenensis* Zhuravlev, *Polygnathus lanei* Kuzmin, *Polygnathus ljascchenkoi* Kuzmin, *Polygnathus pennatus* Hinde, *Polygnathus praepolitus* Kononova, Alekseev, Barskov et Reimers, *Polygnathus uchtensis* Ovnatanova et Kuzmin, and *Polygnathus webbi* Stauffer. *Polygnathus webbi* Stauffer, *Youngquistognathus rossicus* (Zhuravlev) and *Mehlina gradata* Youngquist dominate the conodont association.

Good preservation, low thermal alteration of the conodont elements (CAI=1, i.e. T < 50° C), and the assumed high rate of

lithification of the carbonate host rock (Tarasenko 2011) strongly support the preservation of their near-primary geochemical composition and structure, including organic matter (Rosseeva et al. 2011). Samples were hermetically packed and stored at low temperature (about +5° C) before conodont extraction. Processing of limestone samples followed the standard procedure documented by Harris and Sweet (1989) (dissolution of limestone in 10% buffered acetic acid). The residues were washed through a sieve of 70 µm, dried and conodont elements of genus *Youngquistognathus* (mainly S-elements) were picked up. Sb- and Sc-elements of *Youngquistognathus rossicus* (Zhuravlev) were selected for the study because they are numerous in the collection (about 100 S elements), robust, histologically well-studied, composed of thick lamella, and have various types of hard tissues (Zhuravlev 2003). Eight conodont elements were examined by the microprobe analysis. The specimens were mounted in the low molecular weight epoxy resin based on Bis A (CHS-EPOXY 520) (Sr 0.00%, Ca 0.04%, P 0.21%), ground and polished. The grinding process used Diamond grinding discs UltraPrep (Buehler) before polishing with 0.05 µm MasterPrep Sol-gel alumina suspension (~8.5 pH). The polished surface was cleaned in the ultrasonic cleaner bath for 30 min. The polished slab was coated in Cr for sample conductivity in the electron microprobe. Geochemical analyses were performed using a VEGA TESCAN microprobe (Institute of Geology Komi SC UrB RAS). Five chemical elements (Ca, Sr, Na, P, and F) were analyzed per counting cycle at an accelerating voltage of 20 kV, emission current of 78-88 mA, and a probe diameter of 193-293 nm.

Sample standards include wollastonite for Ca; GaP for P; fluorite for F; SrF₂ for Sr; and albite for Na. All the concentrations are recalculated into weight %.

Microprobe profiles were made up with steps varying from 200 nm up to 390 nm and successive calculation of the central moving average (6 points window width); each profile comprises 100-200 spots. The profiles scan lamellar and paralamellar tissues where oriented across the lamellae (Fig. 3).

RESULTS

Three main hard tissues (lamellar, paralamellar, and albid) were examined by microprobe in different parts of the longitudinal section of Sb-element of *Youngquistognathus rossicus* (Fig. 3a). The results are listed in Tab. 2.

The lamellar tissue is composed of crystallites of calcium phosphate aligned on prismatic and pinacoidal crystal faces. The lattice parameters of the lamellar tissue apatite (a = 9.365-9.37, c = 6.880-6.91 Å) and Ca/P ratio (2.11) are far from those of stoichiometric apatite (CaF) (Wright 1989, 1990;

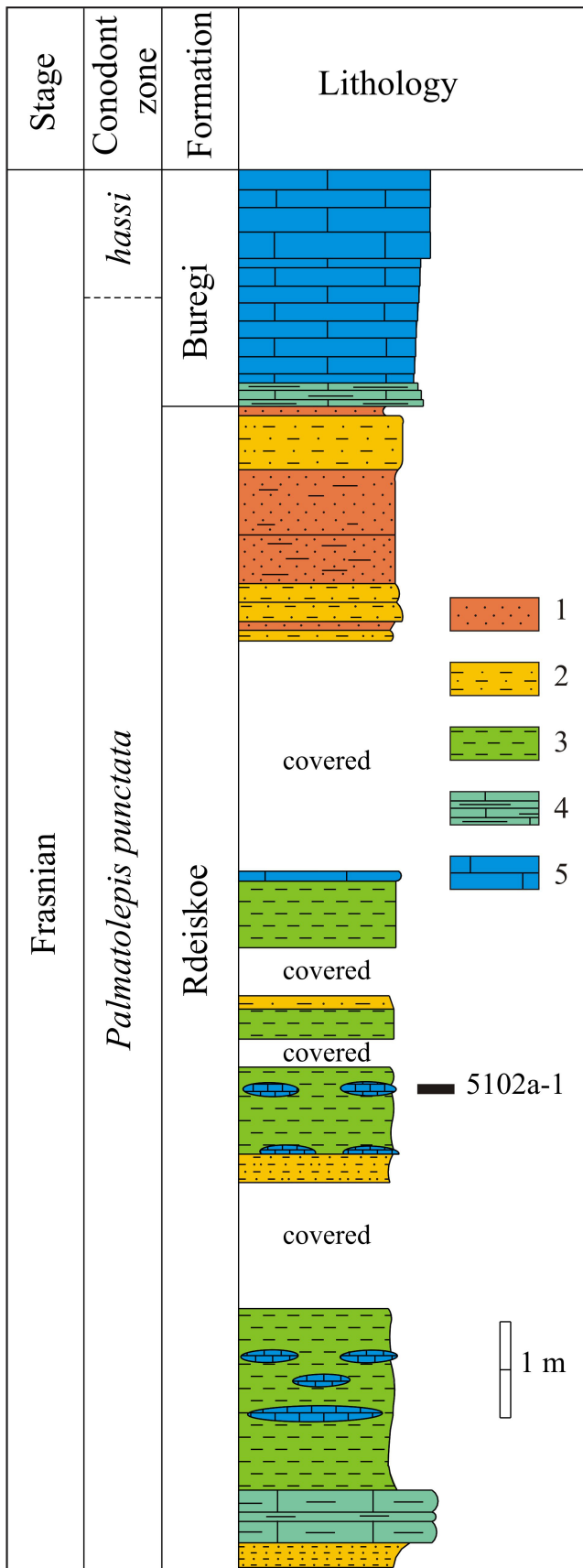


Fig. 2 - Stratigraphical position of the studied sample (5102a-1).
Legend: 1 – sandstone; 2 – siltstone; 3 – claystone; 4 – clayey limestone; 5 – detritic limestone.

Zhuravlev & Sapega 2007), lamellar tissue demonstrates clear lamellar structure, each lamella is 0.6–4 μm thick and comprises a set of slightly disordered crystallites (0.2–0.6 μm thick and 0.6–4 μm long), with c-axis oriented subparallel or oblique to the surface of lamella in the denticles, and subperpendicular to the surface of lamella in the platforms (Fig. 4) (Lindström & Ziegler 1971; Wright 1990). It is believed that crystallite orientation is dependent on the superposition of conodont element surface and secretory epithelium cells. Organic matter of the lamellar tissue composed by collagen-like protein (SDS PAGE data, Rosseeva et al. 2011) forms thin films on the boundaries of crystallites, total content of organic matter is about 3–4 vol.%. The occurrence of collagen in this tissue type was earlier documented by histochemical (Kemp 2002; Gerasimova et al. 2015; Zhuravlev & Gerasimova 2015) and XRD studies (Zhuravlev & Sapega 2007).

The BSE images of the lamellar tissue demonstrate its heterogeneity (Fig. 3b, c). Stripes of various tones elucidate the lamellar structure of the tissue: the couplet of dark and bright stripes corresponds to a single lamella. According to the microprobe analyses the bright stripes composing the outer part of a lamella correspond to slightly increased content of Sr (0.4 wt.% in contrast of 0.19 wt.% in dark stripes). This observation is confirmed by the microprobe profile (Fig. 5) demonstrating periodical oscillation of the Sr content across the lamellae. Sr/Ca ratio (in weight) in the lamellar tissue varies from 0.003 up to 0.011.

Similar distribution of Sr is also observed in the paralamellar tissue (Fig. 6). The variations are close to those in the lamellar tissue (0.48 wt.% in outer part of lamella, and 0.22 wt.% in the inner part). However, the Sr/Ca ratio in the paralamellar tissue varies from 0.006 up to 0.02. Concentrations of F are about 5% in this tissue type.

Albid tissue is composed of micrometer-sized crystallite subunits with preferable crystallographic orientation parallel to the long axis of the denticle (Wright 1990; Rosseeva et al. 2011). These subunits compose porous mesocrystal, appeared as a monocrystal in electron diffraction and cross-polarized light (Rosseeva et al. 2011; Zhuravlev & Gerasimova 2015). The lattice parameter of albid tissue apatite ($a = 9.374\text{--}9.376$, $c = 6.882\text{--}6.892$ Å) and Ca/P ratio (2.04–2.14 in weight) are very close to those of stoichiometric synthetic F-apatite (Frank-Kame-

# point	Tissue type	Na	Ca	P	F	Sr	Sr/Ca	Ca/P
c1	lamellar	0.70	35.2	16.44	4.7	0.3	0.009	2.14
c2	lamellar	0.55	35.2	16.65	4.7	0.4	0.011	2.11
c3	paralamellar	0.55	35.3	16.62	5.0	0.7	0.020	2.12
c4	albid (pore)	0.27	32.7	15.73	5.2	0.4	0.012	2.08
c5	albid	0.21	36.3	17.19	4.3	0.0	0.000	2.11
d1	lamellar	0.58	34.9	16.60	4.0	0.1	0.003	2.10
d2	paralamellar	0.86	34.4	16.57	4.7	0.3	0.009	2.07
d3	paralamellar	0.70	34.6	16.32	5.6	0.2	0.006	2.12
d4	albid	0.15	35.1	16.87	5.0	0.1	0.003	2.08
d5	albid/paralamellar boundary	0.24	33.8	16.14	4.2	0.2	0.006	2.09

Tab. 2 - Microprobe data from different tissue types. Points' numbers correspond to Fig. 3 c, d. Concentrations in wt%.

netskaya et al. 2008). The albid tissue contains Sr of 0.0-0.4 wt.% and F of 4.3-5.2 wt.%. It is supposed that Sr enters the apatite (CaF) structure to replace Ca (Frank-Kamenetskaya et al. 2008).

DISCUSSION

The mean concentrations of Sr in main tissues of conodont element crown agree with previous published results (Tab. 1). However, the previous studies had reported a lack of regular pattern in distribution of Sr concentrations in the tissues of conodont elements (e.g. Pietzner et al. 1968; Wright 1989; Katvala & Henderson 2012). It is most likely related to technical issues, as electron microprobe analyses have been performed in widely spaced spots (about 6000 nm, Katvala & Henderson 2012), that prevent detecting oscillations of 3000-5000 nm scale.

Despite of low spatial resolution, the data by Wright (1989) demonstrate variations in Sr content in the lamellar tissue that are similar to those of the current study. Bright stripes on the BSE image (Wright 1989, pl. 2) have higher Sr content (0.42-0.47%) (Wright 1989, fig. 3, points 4, 20, 28), but darker parts of lamellae have lower Sr content (0.27-0.38%) (Wright 1989, fig. 3, points 5, 6, 27).

The nature of the periodical/cyclic variations in Sr content observed in the lamellar and paralamellar tissues is unclear. It is possible that they might be attributed to the postmortem differential uptake of Sr by the conodont element. On the other hand, they may correlate with variations in the hard tissue permeability caused by nanoporosity. The nanopores (<50 nm) in lamellar tissue are isolated and arranged along the lamella (Trotter et al. 2007: Fig. 2D). Iso-

lated micropores occur in the paralamellar and albid tissues as well (Fig. 3d, e). The arrangement of nano- and micropores suggests that the permeability across lamella is low in both the lamellar and paralamellar tissues, but the permeability along lamella is higher. The low permeability prevents uptake of the external matter into conodont element through its surface. In the attachment area (Fig. 4), all the lamellae composing conodont element crown are exposed and in contact with the host rock. Lateral parts of lamellae, which are exposed in the attachment area, have higher potential as way for uptake of contaminants into conodont element; observed Sr variations demonstrate independence of the distance from the attachment surface. Similar variations occur near the attachment surface (Fig. 3d, e; Fig. 6), and far from the attachment surface (Fig. 3b, c; Fig. 5), contamination along the lamellae is therefore unlikely. Also, the host rock, which may be a source of Sr, demonstrates extremely low content of Sr (0.02-0.04 wt.%). Thus, the post-mortem contamination is also unlikely.

Explanation of variations of Sr concentrations by in vivo processes must take into account peculiarities of the growth of conodont elements. The most realistic model of conodont element growth was elaborated by Bengtson (1976, 1980, 1983) and suggested that the conodont element was retracted in the pocket of the secreting epithelium when not in use, where additive growth occurred during that time. When the conodont element was in use, it extruded from the pocket, and growth stopped. Thus alternation of periods of growth and active functioning was characteristic for conodont elements. The boundaries of lamella, where Sr increase is observed, correspond to arrested growth. Accordingly, several possible causes of such distribution of Sr can be proposed.

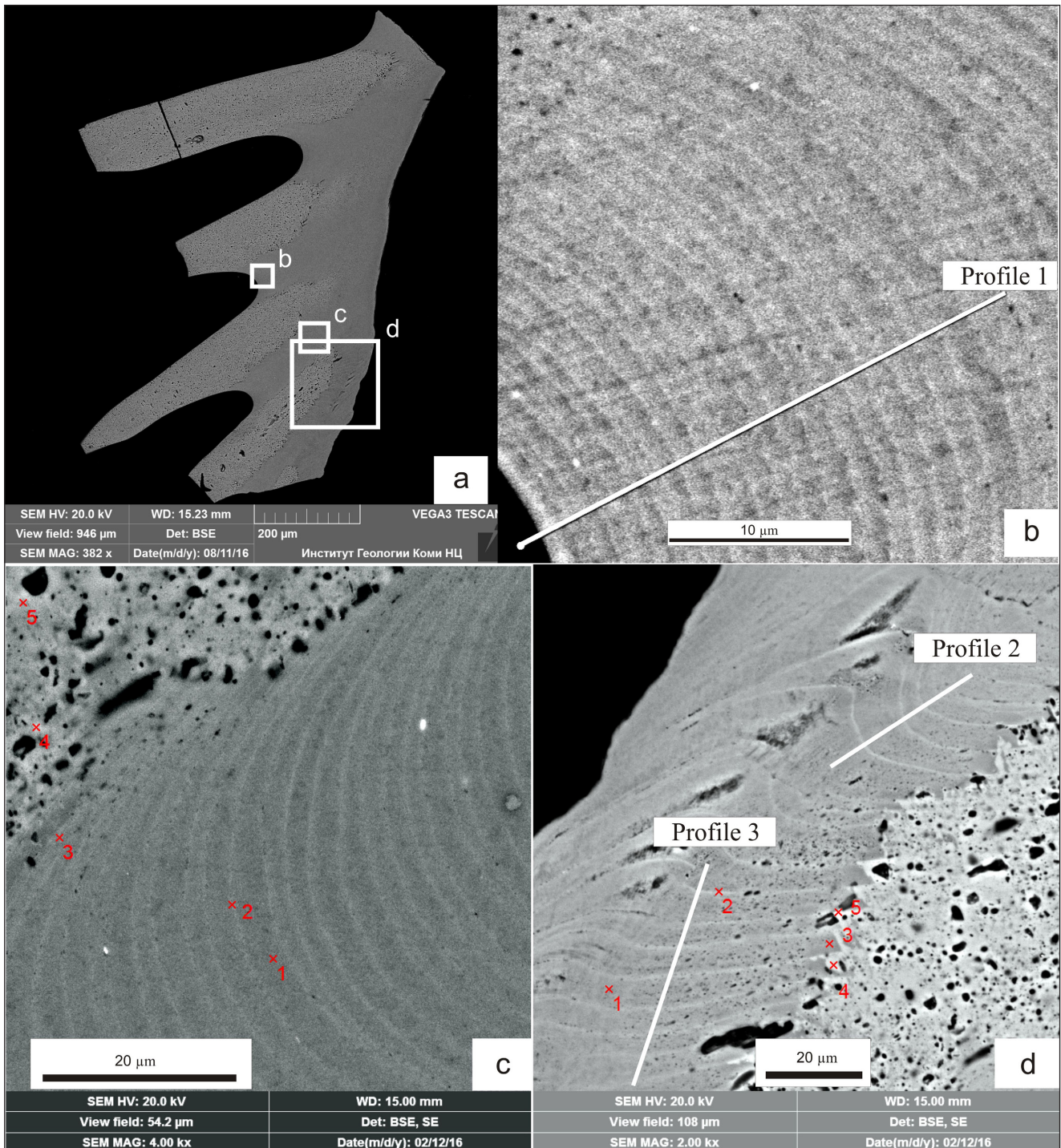


Fig. 3 - BSE image of Sb-element of the conodont *Youngquistognathus rossicus* (Zhuravlev): a - general view; b - close up of a lamellar tissue with microprobe profile (white line); c - lamellar tissue with microprobe spots marked with red crosses; d - paralamellar and albid tissues with microprobe spots marked with red crosses and microprobe profiles (white lines).

One possibility would be that ambient sea water, in contact with the surface of conodont elements when functioning, was source of Sr in the conodont hard tissue. If so, the outer layer of conodont elements became enriched by Sr. The oscillation of the Sr concentrations can be also explained by the model of hard tissues formation (Zhuravlev & Gerasimova

2015). According to this model, each growth cycle produced a couplet of lamellae, where the inner lamella composed of lamellar, paralamellar, or albid tissue, and the outer lamella composed of lamellar tissue. The cycle consists of five stages (Zhuravlev & Gerasimova 2015): 1) partial resorption of the outer lamella; 2) formation of the organic matrix of

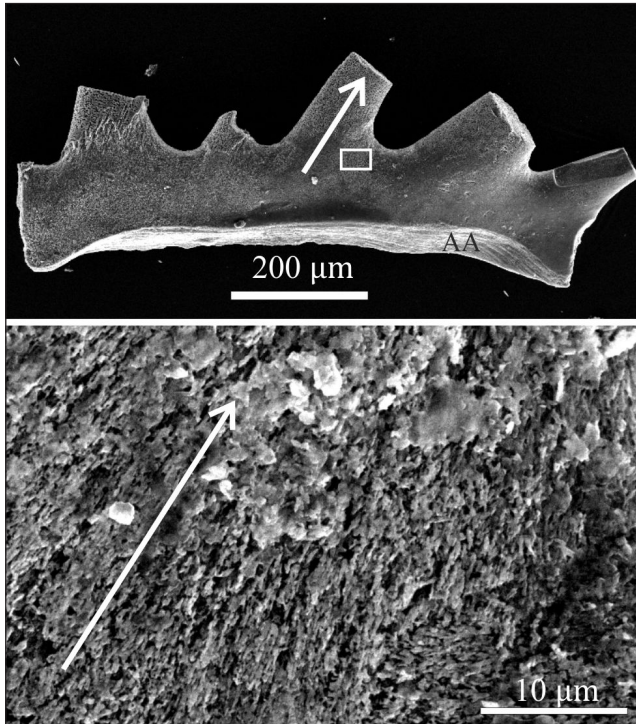


Fig. 4 - Orientation of the crystallites in the lamellar tissue of Sb element of *Youngquistognathus rossicus* (Zhuravlev) (etched lateral surface of the denticle). White arrow marks the denticle axis.

the new lamellae; 3) initial crystallization of the disordered crystallites of the lamella; 4) recrystallization of the crystallites around the organic matrix; and 5) formation of the new outer lamella composed of la-

mellar tissue. The outer lamella probably absorbed Sr from the sea water, where the Sr/Ca ratio is much higher than that in the conodont tissue (about 0.03, Castro & Huber 2003). Successive resorption of the outer lamella during the next growth cycle partly eliminates the Sr-enriched tissue. The residue of this tissue composes a thin layer at the boundary of the lamellae having high Sr concentrations. High Sr concentration in the outer lamella of the conodont elements here studied (Fig 3b; Fig. 5) supports this model.

There is a third possible mechanism of enriching Sr, analogous with enamel of vertebrates, where the highly mineralized hard tissue has similarity in composition and structure with the lamellar tissue of conodonts (Donoghue et al. 2000; Rosseeva et al. 2011; Katvala & Henderson 2012). Demineralization of the vertebrate enamel induces an increase of Sr with respect to Ca, attributed to partial bioapatite dissolution and/or to chelate extraction and concentration of trace metals (Preoteasa et al. 2008). A similar process might have occurred during the conodont element resorption at the first stage of the growth cycle. The residue of the outer lamella can be enriched by Sr by selective extraction of Ca during the resorption.

In any case, the distribution pattern of Sr in conodont lamellar (paralamellar) tissue differs from its counterpart in the enamel. The Sr distribution in enamel does not reflect the pattern of incremental lines (Alvira et al. 2011), elucidating difference in

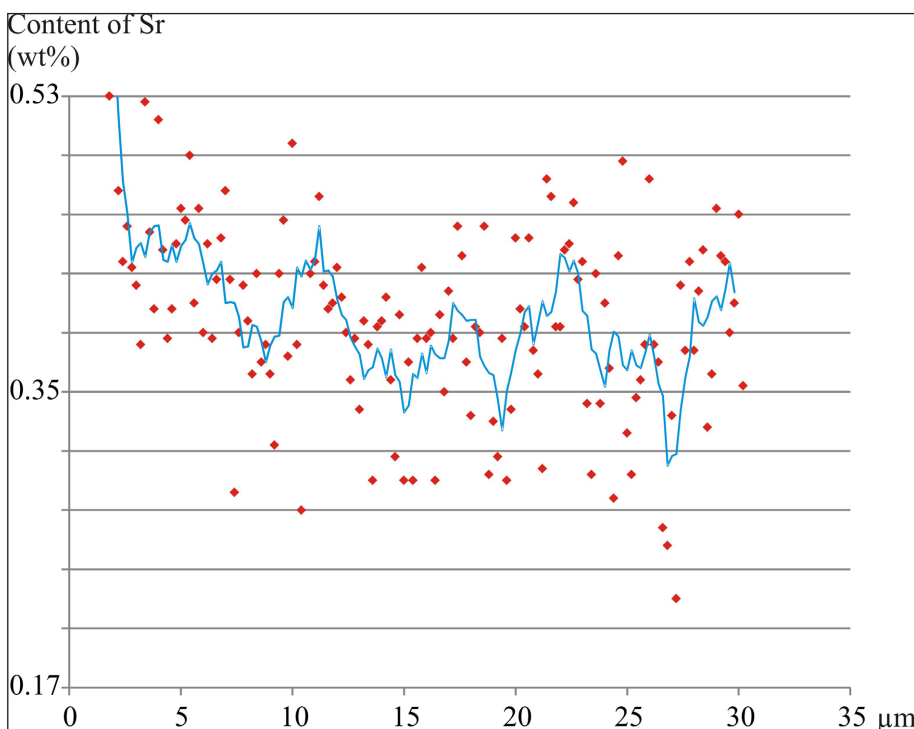
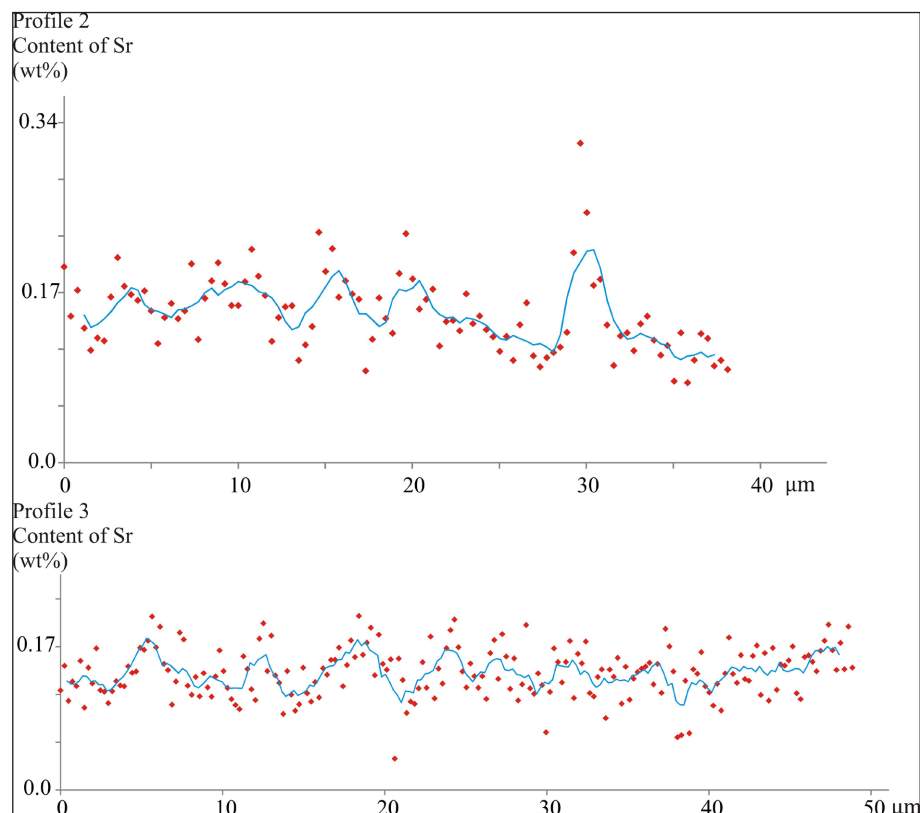


Fig. 5 - Microprobe profile of the lamellar tissue. The studied area corresponds to the Fig. 3b.

Fig. 6 - Microprobe profiles of the paramellar tissue. The studied area and profiles' numbers corresponds to the Fig. 3d.



growth modes of conodont tissues and enamel.

Distances between the Sr-enriched layers (in transverse section of conodont element) in the lamellar and paramellar tissues reflect thickness of the lamella. The lamella thickness is proportional to growth rate of corresponding part of a conodont element (e.g., Dzik 2008). Thus, average Ca/Sr ratio in the lamellar and paramellar tissue can be used as a proxy of growth rate of conodont element. Application of this ratio for comparative investigation of the growth rates of elements of different conodont taxa is feasible.

CONCLUSIONS

The lamellar and paramellar tissues of conodont element crown Sr concentrations demonstrate oscillations correlated with the periodic growth of the lamellae. The maximum Sr content is observed near the lamella boundaries (about 0.4 wt % in contrast to 0.19 wt % far from the lamella boundary). It is suggested that the distribution pattern of Sr in the lamellar and paramellar tissues was most likely controlled by biomineralization including partial resorption of the outer part of lamella during the growth cycle. The albid tissue of the internal parts of conodont ele-

ments shows minor or no Sr contents.

The distribution pattern of Sr in conodont hard tissues differs from its counterpart in the enamel of vertebrates. These results combined with morphologic and crystallographic characteristics of lamellar and paramellar tissues support a lack of homology in the enamel of vertebrates.

Acknowledgements. The authors would like to thank the editor and referees for their constructive reviews and editing of the manuscript.

REFERENCES

- Alvira F., Ramirez R.F., Torchia G., Roso L. & Bilmes G. (2011) - A new method for relative Sr determination in human teeth enamel. *J. Anthropol. Sci.*, 89: 153-160.
- Bengtson S. (1976) - The structure of some Middle Cambrian conodonts, and the early evolution of conodont structure and function. *Lethaia*, 9: 185-206.
- Bengtson S. (1980) - Conodonts: the need for a functional model. *Lethaia*, 13: 320.
- Bengtson S. (1983) - A functional model for the conodont apparatus. *Lethaia*, 16: 38.
- Blick A., Turner S., Burrow C. J., Schultze H.-P., Rexroad C.B., Bultynck P. & Nowlan G.S. (2010) - Fossils, histology, and phylogeny: why conodonts are not vertebrates. *Episodes*, 33(4): 234-241.
- Castro P. & Huber M. E. (2003) - Marine Biology. 4th ed. Mc-

- Graw Hill, Boston, 480 pp.
- Donoghue P. C. J. (1998) - Growth and patterning in the conodont skeleton. *Phil. Trans. R. Soc. Lond., B*, 353: 633-666.
- Donoghue P. C. J., Forey P. L. & Aldridge R. J. (2000) - Conodont affinity and chordate phylogeny. *Biol. Rev.*, 75: 191-251.
- Dzik J. (2008) - Evolution of morphogenesis in 360-million-year-old conodont chordates calibrated in days. *Evol. Dev.*, 10(6): 769-777.
- Frank-Kamenetskaya O. V., Rozhdestvenskaya I. V., Rosseeva E. V. & Zhuravlev A. V. (2014) - Refinement of Apatite Atomic Structure of Albid Tissue of Late Devon Conodont. *Crystallogr. Rep.*, 59(1): 41-47.
- Gerasimova A. I., Zhuravlev A. V. & Rosseeva E. V. (2015) - Structure and origin of the albid tissue of conodonts. In: Canoville A., Mitchell J., Stein K., Konietzko-Meier D., Teschner E., van Heteren A. & Sander P.M. (Eds) - 3rd SPH Program and Abstract Book: 81. Steinmann Institute, University of Bonn, Bonn.
- Harris A.G. & Sweet W.C. (1989) - Mechanical and chemical techniques for separating microfossils from rock. Sediment and residue matrix. In: Feldmann R.M., Chapman R.E. & Hannibal J.T. (Eds) - Paleotechniques: 70-86. *Paleontol. Soc. Spec. Publ.*, 4.
- Holmden C., Creaser R.A., Muehlenbachs K., Bergström S.M. & Leslie S.A. (1996) - Isotopic and elemental systematics of Sr and Nd in 454 Ma biogenic apatites: implications for paleoseawater studies. *Earth Planet. Sci. Lett.*, 142: 425-437.
- Kasatkina A. P. & Buryi G. I. (1996) - On the relation of chaetognaths and conodonts. *Albertiana*, 18: 21-23.
- Katvala E.C. & Henderson C.M. (2012) - Chemical element distributions within conodont elements and their functional implications. *Paleobiology*, 38: 447-458. doi:10.1666/11038.1.
- Kemp A. (2002) - Aminoacid residues in conodont elements. *J. Paleontol.*, 76: 518-528.
- Klapper G. (1997) - Graphic correlation of Frasnian (Upper Devonian) sequences in Montagne Noire, France, and western Canada. *Geol. Soc. Spec. Pap.*, 321: 113-129.
- Kürschner W., Becker R.T., Buhl D. & Veizer J. (1992) - Strontium isotopes in conodonts: Devonian-Carboniferous transition, the northern Rhenish Slate Mountains, Germany. *Ann. Soc. géol. Belg.*, 115(2): 595-621.
- Müller K. J. & Nogami Y. (1971) - Über den Feinbau der Conodonten. *Mem. Fac. Sci. Kyoto Univ., Ser. Geol. Miner.*, 38: 1-88.
- Pietzner H., Vahl J., Werner H. & Ziegler W. (1968) - Zur chemischen Zusammensetzung und mikromorphologie der conodonten. *Palaeontogr. Abt. A*, 128(4-6): 115-152.
- Preoteasa E.A., Preoteasa E., Kuczumow A., Gurban D., Harangus L., Grambole D. & Herrmann F. (2008) - Broad-beam PIXE and m-PIXE analysis of normal and in vitro demineralized dental enamel. *X Ray Spectrom.*, 37: 517-535. DOI: 10.1002/xrs.1083
- Rosseeva E., Borrmann H., Cardoso-Gil R., Carrillo-Cabrera W., Frank-Kamenetskaya O. V., Öztan Y., Prots Y., Schwarz U., Simon P., Zhuravlev A. V. & Kniep R. (2011) - Evolution and Complexity of Dental (Apatite-Based) Biominerals: Mimicking the Very Beginning in the Laboratory: 171-176. Max-Planck-Institut für Chemische Physik fester Stoffe, Scientific Report 2009-2010.
- Tarasenko A. B. (2011) - Tempestite Beds in the Ilmen Clays of the Frasnian Stage of the Main Devonian Field (North-West of the East European Platform). *Uchenye Zapiski Kazanskogo Universiteta. Seriya Estestvennyye Nauki*, 153(4): 260-266 [in Russian].
- Trotter J.A., Barnes C.R. & McCracken A.D. (2016) - Rare earth elements in conodont apatite: Seawater or pore-water signatures? *Palaeogeogr., Palaeoclimatol., Palaeoecol.*, 462: 92-100.
- Trotter J.A. & Eggins S.M. (2006) - Chemical systematics of conodont apatite determined by laser-ablation ICPMS. *Chem. Geol.*, 233: 196-216.
- Trotter J.A., Fitz Gerald J.D., Kokkonen H. & Barnes C.R. (2007) - New insights into the ultrastructure, permeability, and integrity of conodont apatite determined by transmission electron microscopy. *Lethaia*, 40: 97-110.
- Trotter J.A., Korsch M.J., Nicoll R.S. & Whitford D.J. (1999) - Sr isotopic variation in single conodont elements: implications for defining the Sr seawater curve. In: Serpagli E. (Ed.) - Seventh European Conodont Symposium. Studies on Conodonts: 507-514. *Boll. Soc. Paleontol. It.*, Bologna-Modena.
- Turner S., Burrow C. J., Schultze H.-P., Blicek A., Reif W.-E., Rexroad C. B., Bultynck P. & Nowlan G. S. (2010) - False teeth: conodont-vertebrate phylogenetic relationships revisited. *Geodiversitas*, 32(4): 545-594.
- Wright J. (1989) - Conodont Apatite: Structure and Geochemistry. In: Carter G. (Ed.) - Skeletal Biomineralization: Patterns, Processes and Evolutionary Trends: 149-163. American Geophysical Union, Washington, D. C. doi: 10.1029/SC005p0149
- Wright J. (1990) - Conodont geochemistry: a key to the Palaeozoic. *Cour. Forsch.-Inst. Senckenberg*, 118: 227-305.
- Zhuravlev A.V. (2002) - A new type of conodont hard tissue. *Lethaia*, 35(3): 275-276.
- Zhuravlev A.V. (2003) - Micro-reticulation and internal composition of the elements of the apparatus of "Polygnathus" rossicus Zhuravlev (Conodonta, Late Devonian, Frasnian). *Neues Jahrb. Geol. Paläontol. Mb.*, 2: 120-128.
- Zhuravlev A., Evdokimova I. & Sokiran E. (1997) - New data on conodonts, brachiopods, and ostracodes from the stratotypes of the Ilmen and Buregi Beds (Frasnian, Main Devonian Field). *Proc. Estonian Acad. Sci. Geol.*, 46(4): 169-186.
- Zhuravlev A.V. & Sapega V.F. (2007) - XRD data on composition of the hard tissues of the Late Palaeozoic conodonts. In: Bio-Inert Interactions: Life and Rocks. Materials of the 3rd International Symposium: 63-64. VSEGEI, St. Petersburg [in Russian].
- Zhuravlev A.V., Sokiran E.V., Evdokimova I.O., Dorofeeva L.A., Rusetskaya G.A. & Malkowski K. (2006) - Faunal and facies changes at the Early-Middle Frasnian boundary in the north-western East European Platform. *Acta Palaeontol. Pol.*, 51(4): 747-758.
- Zhuravlev A.V. & Gerasimova A.I. (2015) - Albid tissue of the conodont elements: composition and forming model. *Vestnik IG*, 10(250): 21-27 [in Russian, English abstract].